Central Crack in a Piezoelectric Disc

Jong Ho Kwon*
Department of Automotive Engineering, ShinHeung College
117 Howon-dong, Uijeongbu, Gyeonggi 480-701, Korea

This study is concerned with the general solution of the field intensity factors and energy release rate for a Griffith crack in a piezoelectric ceramic of finite radius under combined anti-plane mechanical and in-plane electrical loading. Both electrically continuous and impermeable crack surface conditions are considered. Employing Mellin transforms and Fourier series, the problem is reduced to dual integral forms. The solution to the resulting expressions is expressed in terms of Fredholm integral equation of the second kind. The solutions are provided to study the influence of the crack length, the crack surface boundary conditions on the intensity factors and the energy release rate.

Key Words: Piezoelectric Disc, Central Crack, Crack Boundary Condition, Intensity Factors, Energy Release Rate, Integral Transform

1. Introduction

Piezoelectric materials, such as lead zirconate titanate ceramics (PZT) possess high degree of linearity, high power density, greater efficiency and potential for low cost manufacture in comparison with alternative electromechanically coupled materials. Indeed, the creative application of piezoelectric materials in engineering has given rise to the remarkable progress in the development of sensors and actuators in smart structures. Piezoceramic actuators and sensors have been used in smart structures to obtain precision positioning, vibration suppression, and noise control. However, piezoceramic materials contain micro and macrodefects and behave in a brittle fashion. Because the performance of piezoelectric devices is affected by these defects, a number of studies have been performed ; see, e.g., the works of Deeg (1980), McMeeking (1989), Pak (1990), Sosa (1991), Park and Sun (1995), Shindo et al.(1996, 1997), Meguid and Wang (1998), Wang and Meguid (2001), Kwon and Lee (2000, 2001), and Kwon and Meguid (2002).

To effectively design and fabricate piezoelectric actuators and sensors, their behaviour must be evaluated and understood under conditions simulating their operating environments. In many practical applications, especially in sensor technologies, piezoelectric ceramics can be produced in many shapes and include discs, plates, tubes, rings, washers, hemispheres, and spherical elements. Some attention has been focused on the crack problem in a rectangular piezoelectric material ; see, e.g., Kwon and Lee (2000, 2001). However, the crack problem in a piezoelectric disc or cylinder has not been given its due attention. In addition, the electric boundary condition along the crack surface of piezoelectric materials is still an open problem. The permeable or continuous condition implies that the normal component of electric displacement and the tangential component of electric field should be continuous across the crack surface. Recently, Zhang et al. (1998), Narita and Shindo (1998) and Gao and Fan (1999) argued the validity of this condition. In contrast, Pak and Goloubeva (1996), Zhao et al.(1997), Liu et al.(1998) and Qin and Mai

* **E-mail** : jkwon@shc.ac.kr
TEL : +82-31-870-3644; **FAX** : +82-31-870-3646
Department of Automotive Engineering, ShinHeung College, 117 Howon-dong, Uijeongbu, Gyeonggi 480-701, Korea. (Manuscript **Received** October 22, 2003; **Revised** May 18, 2004)

(1999) used the impermeable crack condition. It is for these reasons that I offer the current study.

In the present paper, the field intensity factors and energy release rate are provided for a Griffith crack in a circular piezoelectric ceramic under combined anti-plane mechanical and in-plane electrical loading. Two problems of the electrically continuous and impermeable crack surface conditions are considered. The problems are reduced to the forms of dual integral equations by use of Mellin transforms and Fourier series, and the solutions are expressed in the terms of Fredholm integral equation of the second kind. Analytical solutions are provided to study the influence of the crack length and the crack surface boundary conditions. Numerical examples of the stress intensity factor, the electric displacement intensity factor and the energy release rate show the dependence of these quantities upon the two different crack surface boundary conditions considered in the study.

2. Fundamental Relations and Problem Statements

Consider a circular piezoelectric ceramic of radius R containing a Griffith crack of length $2a$ at its centre, as shown in Figure 1. It is assumed that the anti-plane shear stress $\tau(r)=\tau_0$ and the in-plane electric displacement $D(r)=D_0$ act on the crack surfaces, as depicted in Figure 1.

In this case, the mechanical displacements and electric fields are simplified such as

$$u_r=u_r(r,\theta)=0,\ u_\theta=u_\theta(r,\theta)=0,\ u_z=u_z(r,\theta) \quad (1)$$

$$E_r=E_r(r,\theta),\ E_\theta=E_\theta(r,\theta),\ E_z=E_z(r,\theta)=0 \quad (2)$$

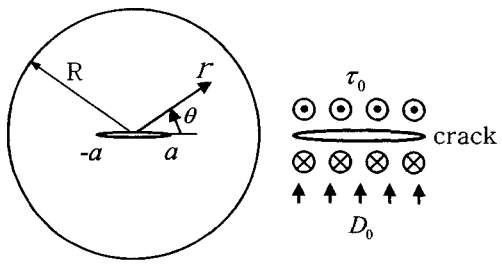

Fig. 1 A central crack in a piezoelectric disc

Therefore, the constitutive relations for this problem can be expressed in the cylindrical co-ordinates system as:

$$\gamma_{zr}(r,\theta)=\frac{\partial}{\partial r}u_z(r,\theta),\ \gamma_{z\theta}(r,\theta)=\frac{\partial}{r\partial\theta}u_z(r,\theta) \quad (3)$$

$$E_r(r,\theta)=-\frac{\partial}{\partial r}\varphi(r,\theta),\ E_\theta(r,\theta)=-\frac{\partial}{r\partial\theta}\varphi(r,\theta) \quad (4)$$

$$\tau_{zj}(r,\theta)=c_{44}\gamma_{zj}(r,\theta)-e_{15}E_j(r,\theta) \quad (5)$$

$$D_j(r,\theta)=e_{15}\gamma_{zj}(r,\theta)+\varepsilon_{11}E_j(r,\theta) \quad (6)$$

where $j=r,\ \theta$. Also, $u_z(r,\theta)$, $\varphi(r,\theta)$, $E_j(x,y)$, and $D_j(x,y)$ are the mechanical displacements, electric potentials, electric fields and electric displacements, respectively. The coefficients c_{44}, e_{15} and ε_{11} are the elastic stiffness, the piezoelectric constants and the dielectric constants of the piezoelectric materials, respectively.

In the cylindrical co-ordinates system, the respective equilibrium equation and the equation of electrostatics are expressed as

$$\frac{\partial}{\partial r}\tau_{zr}+\frac{\partial}{r\partial\theta}\tau_{z\theta}+\frac{1}{r}\tau_{zr}=0 \quad (7)$$

$$\frac{\partial}{\partial r}D_r+\frac{\partial}{r\partial\theta}D_\theta+\frac{1}{r}D_r=0 \quad (8)$$

From Eqs. (5)~(8), the anti-plane governing equations for the present boundary value problem become

$$c_{44}\nabla_c^2u_z(r,\theta)+e_{15}\nabla_c^2\varphi(r,\theta)=0 \quad (9)$$

$$e_{15}\nabla_c^2u_z(r,\theta)-\varepsilon_{11}\nabla_c^2\varphi(r,\theta)=0 \quad (10)$$

where $\nabla_c^2=\frac{\partial^2}{\partial r^2}+\frac{\partial^2}{r^2\partial\theta^2}+\frac{\partial}{r\partial r}$.

By considering the geometry and electromechanical loading, the following boundary conditions should be satisfied:

$$\left.\begin{array}{l}\tau_{zr}(R,\theta)=0\ (0\le\theta<2\pi)\\ D_r(R,\theta)=0\ (0\le\theta<2\pi)\end{array}\right\} \quad (11)$$

As indicated in the introduction, the crack surface boundary conditions of piezoelectric materials have been studied by numerous investigators, and remain a subject of contention. In this study, we consider the following two combinations of the mixed boundary conditions:

Mechanical mixed boundary conditions

$$\left.\begin{array}{ll}\tau_{z\theta}(r,0)=-\tau(r)=-\tau_0 & (|r|<a)\\ u_z(r,0)=0 & (a<|r|\le R)\end{array}\right\} \quad (12)$$

(i) Electrical mixed boundary conditions based on continuous crack surface

$$\left.\begin{array}{ll}D_\theta(r,0^+)=D_\theta(r,0^-)=0 & (|r|<a)\\ E_r(r,0^+)=E_r(r,0^-) & (|r|<a)\\ \varphi(r,0)=0 & (a<|r|\le R)\end{array}\right\} \quad (13)$$

(ii) Electrical mixed boundary conditions based on impermeable crack surface

$$\left.\begin{array}{ll}D_\theta(r,0)=-D(r)=-D_0 & (|r|<a)\\ \varphi(r,0)=0 & (a<|r|\le R)\end{array}\right\} \quad (14)$$

3. Analytical Solution Procedure

The mechanical displacement and electric potential can be described from the governing equations ((9) and (10)) by applying the Mellin transforms and Fourier series; as follows:

$$u_z(r,\theta)=\frac{1}{2\pi i}\int_{c-i\infty}^{c+i\infty}A_1(s)\cos\left\{\left(\theta-\frac{\pi}{2}\right)s\right\}\frac{r^{-s}}{s\cos\left(\frac{\pi}{2}s\right)}ds + \sum_{n=1,3,\cdots}^{\infty}B_1(n)\,r^n\sin(n\theta) \quad (15)$$

$$\varphi(r,\theta)=\frac{1}{2\pi i}\int_{c-i\infty}^{c+i\infty}A_2(s)\cos\left\{\left(\theta-\frac{\pi}{2}\right)s\right\}\frac{r^{-s}}{s\cos\left(\frac{\pi}{2}s\right)}ds + \sum_{n=1,3,\cdots}^{\infty}B_2(n)\,r^n\sin(n\theta) \quad (16)$$

The field variables are expressed using Eqs. (3) ~ (6), such that

$$\gamma_{zr}(r,\theta)=-\frac{1}{2\pi i}\int_{c-i\infty}^{c+i\infty}A_1(s)\cos\left\{\left(\theta-\frac{\pi}{2}\right)s\right\}\frac{r^{-s-1}}{\cos\left(\frac{\pi}{2}s\right)}ds + \sum_{n=1,3,\cdots}^{\infty}nB_1(n)\,r^{n-1}\sin(n\theta) \quad (17)$$

$$\gamma_{z\theta}(r,\theta)=-\frac{1}{2\pi i}\int_{c-i\infty}^{c+i\infty}A_1(s)\sin\left\{\left(\theta-\frac{\pi}{2}\right)s\right\}\frac{r^{-s-1}}{\cos\left(\frac{\pi}{2}s\right)}ds + \sum_{n=1,3,\cdots}^{\infty}nB_1(n)\,r^{n-1}\cos(n\theta) \quad (18)$$

$$E_r(r,\theta)=\frac{1}{2\pi i}\int_{c-i\infty}^{c+i\infty}A_2(s)\cos\left\{\left(\theta-\frac{\pi}{2}\right)s\right\}\frac{r^{-s-1}}{\cos\left(\frac{\pi}{2}s\right)}ds - \sum_{n=1,3,\cdots}^{\infty}nB_2(n)\,r^{n-1}\sin(n\theta) \quad (19)$$

$$E_\theta(r,\theta)=\frac{1}{2\pi i}\int_{c-i\infty}^{c+i\infty}A_2(s)\sin\left\{\left(\theta-\frac{\pi}{2}\right)s\right\}\frac{r^{-s-1}}{\cos\left(\frac{\pi}{2}s\right)}ds - \sum_{n=1,3,\cdots}^{\infty}nB_2(n)\,r^{n-1}\cos(n\theta) \quad (20)$$

$$\tau_{zr}(r,\theta)=-\frac{1}{2\pi i}\int_{c-i\infty}^{c+i\infty}[c_{44}A_1(s)+e_{15}A_2(s)]\cos\left\{\left(\theta-\frac{\pi}{2}\right)s\right\}\frac{r^{-s-1}}{\cos\left(\frac{\pi}{2}s\right)}ds + \sum_{n=1,3,\cdots}^{\infty}n[c_{44}B_1(n)+e_{15}B_2(n)]\,r^{n-1}\sin(n\theta) \quad (21)$$

$$\tau_{z\theta}(r,\theta)=-\frac{1}{2\pi i}\int_{c-i\infty}^{c+i\infty}[c_{44}A_1(s)+e_{15}A_2(s)]\sin\left\{\left(\theta-\frac{\pi}{2}\right)s\right\}\frac{r^{-s-1}}{\cos\left(\frac{\pi}{2}s\right)}ds + \sum_{n=1,3,\cdots}^{\infty}n[c_{44}B_1(n)+e_{15}B_2(n)]\,r^{n-1}\cos(n\theta) \quad (22)$$

$$D_r(r,\theta)=-\frac{1}{2\pi i}\int_{c-i\infty}^{c+i\infty}[e_{15}A_1(s)-\varepsilon_{11}A_2(s)]\cos\left\{\left(\theta-\frac{\pi}{2}\right)s\right\}\frac{r^{-s-1}}{\cos\left(\frac{\pi}{2}s\right)}ds + \sum_{n=1,3,\cdots}^{\infty}[e_{15}B_1(n)-\varepsilon_{11}B_2(n)]\,r^{n-1}\sin(n\theta) \quad (23)$$

$$D_\theta(r,\theta)=-\frac{1}{2\pi i}\int_{c-i\infty}^{c+i\infty}[e_{15}A_1(s)-\varepsilon_{11}A_2(s)]\sin\left\{\left(\theta-\frac{\pi}{2}\right)s\right\}\frac{r^{-s-1}}{\cos\left(\frac{\pi}{2}s\right)}ds + \sum_{n=1,3,\cdots}^{\infty}n[e_{15}B_1(n)-\varepsilon_{11}B_2(n)]\,r^{n-1}\cos(n\theta) \quad (24)$$

Using the Fourier sine series pair, Eq. (11) gives the following relations

$$B_k(n)=\frac{4}{\pi}R^{-n}\frac{1}{2\pi i}\int_{c-i\infty}^{c+i\infty}A_k(s)\frac{R^{-s}}{n^2-s^2}ds \quad (k=1,2) \quad (25)$$

3.1 Solution for electrically continuous crack boundary condition

In the case of electrically continuous crack surface condition, the following two pairs of dual integral equations are obtained from Eqs. (12) and (13),

$$\left\{\begin{array}{ll}\dfrac{1}{2\pi i}\dfrac{d}{dr}\displaystyle\int_{c-i\infty}^{c+i\infty}[c_{44}A_1(s)+e_{15}A_2(s)]\frac{r^{-s}}{s}\tan\left(\frac{\pi}{2}s\right)ds & \\ \quad-\displaystyle\sum_{n=1,3,\cdots}^{\infty}n[c_{44}B_1(n)+e_{15}B_2(n)]r^{n-1}=\tau_0 & (|r|<a)\\ \dfrac{1}{2\pi i}\displaystyle\int_{c-i\infty}^{c+i\infty}A_1(s)\frac{r^{-s}}{s}ds=0 & (a<|r|\le R)\end{array}\right\} \tag{26}$$

$$\left\{\begin{array}{l}\dfrac{1}{2\pi i}\dfrac{d}{dr}\displaystyle\int_{c-i\infty}^{c+i\infty}A_2(s)\frac{r^{-s}}{s}ds=0\ (|r|<a)\\ \dfrac{1}{2\pi i}\displaystyle\int_{c-i\infty}^{c+i\infty}A_2(s)\frac{r^{-s}}{s}ds=0\qquad(a<|r|\le R)\end{array}\right\} \tag{27}$$

The solution of Eqs. (26) and (27) can be obtained by introducing the new function $\phi_k(\xi)$ such that:

$$A_k(s)=\frac{\Gamma\left(\frac{1}{2}\right)\Gamma\left(\frac{1}{2}s\right)}{2\Gamma\left(\frac{1}{2}+\frac{1}{2}s\right)}s\int_0^a\xi^s\phi_k(\xi)\,d\xi \tag{28}$$

Making use of Eqs. (27) and (28) leads to the result that $\phi_2(\xi)=0$. And, we can establish that $A_2(s)=B_2(n)=0$ from Eqs. (25) and (28).

Therefore, using Eqs. (25) and (28), the dual integral equations (26) can be rewritten as

$$\left\{\begin{array}{ll}\dfrac{d}{dr}\displaystyle\int_0^a\phi_1(\xi)\prod_1(r,s,\xi)\,d\xi & \\ \quad-\displaystyle\sum_{n=1,3,\cdots}^{\infty}\frac{4}{\pi}nR^{-n}r^{n-1}\int_0^a\phi_1(\xi)\prod_2(r,s,\xi)\,d\xi & \\ =\dfrac{\tau_0}{c_{44}} & (|r|<a)\\ \displaystyle\int_0^a\phi_1(\xi)\prod_3(r,s,\xi)\,d\xi=0 & (a<|r|\le R)\end{array}\right\} \tag{29}$$

where

$$\prod_1(r,s,\xi)=\frac{1}{2\pi i}\int_{c-i\infty}^{c+i\infty}\frac{\Gamma\left(\frac{1}{2}\right)\Gamma\left(\frac{1}{2}s\right)}{2\Gamma\left(\frac{1}{2}+\frac{1}{2}s\right)}\left(\frac{r}{\xi}\right)^{-s}\tan\left(\frac{\pi}{2}s\right)ds \tag{30}$$

$$\prod_2(r,s,\xi)=\frac{1}{2\pi i}\int_{c-i\infty}^{c+i\infty}\frac{\Gamma\left(\frac{1}{2}\right)\Gamma\left(\frac{1}{2}s\right)}{2\Gamma\left(\frac{1}{2}+\frac{1}{2}s\right)}\left(\frac{R}{\xi}\right)^{-s}\frac{s}{n^2-s^2}ds \tag{31}$$

$$\prod_3(r,s,\xi)=\frac{1}{2\pi i}\int_{c-i\infty}^{c+i\infty}\frac{\Gamma\left(\frac{1}{2}\right)\Gamma\left(\frac{1}{2}s\right)}{2\Gamma\left(\frac{1}{2}+\frac{1}{2}s\right)}\left(\frac{r}{\xi}\right)^{-s}ds \tag{32}$$

In addition, the right sides of Eqs. (30)~(32) can be respectively expressed as (see Appendix for details):

$$\frac{1}{2\pi i}\int_{c-i\infty}^{c+i\infty}\frac{\Gamma\left(\frac{1}{2}\right)\Gamma\left(\frac{1}{2}s\right)}{2\Gamma\left(\frac{1}{2}+\frac{1}{2}s\right)}\left(\frac{r}{\xi}\right)^{-s}\tan\left(\frac{\pi}{2}s\right)ds=\left\{\begin{array}{ll}0 & :|r|<\xi\\ \dfrac{\xi}{\sqrt{r^2-\xi^2}} & :|r|>\xi\end{array}\right\} \tag{33}$$

$$\frac{1}{2\pi i}\int_{c-i\infty}^{c+i\infty}\frac{\Gamma\left(\frac{1}{2}\right)\Gamma\left(\frac{1}{2}s\right)}{2\Gamma\left(\frac{1}{2}+\frac{1}{2}s\right)}\left(\frac{r}{\xi}\right)^{-s}\frac{s}{n^2-s^2}ds=-\frac{\Gamma\left(\frac{1}{2}\right)\Gamma\left(\frac{1}{2}n\right)}{4\Gamma\left(\frac{1}{2}+\frac{1}{2}n\right)}\left(\frac{R}{\xi}\right)^{-n} \tag{34}$$

$$\frac{1}{2\pi i}\int_{c-i\infty}^{c+i\infty}\frac{\Gamma\left(\frac{1}{2}\right)\Gamma\left(\frac{1}{2}s\right)}{2\Gamma\left(\frac{1}{2}+\frac{1}{2}s\right)}\left(\frac{r}{\xi}\right)^{-s}ds=\left\{\begin{array}{ll}\dfrac{\xi}{\sqrt{\xi^2-r^2}} & :|r|<\xi\\ 0 & :|r|>\xi\end{array}\right\} \tag{35}$$

Substituting Eqs. (30)~(35) into Eq. (29), the unknown function $\phi_1(\xi)$, for an electrically continuous crack condition, should satisfy the Fredholm integral equation of the second kind and take the form,

$$\phi_1(\xi)+\int_0^a\phi_1(\eta)\left\{\frac{1}{\pi}\sum_{n=1,3,\cdots}^{\infty}n\left[\frac{\Gamma\left(\frac{1}{2}n\right)}{\Gamma\left(\frac{1}{2}+\frac{1}{2}n\right)}\right]^2\frac{\eta^n}{R^{2n}\xi^{n-1}}\right\}d\eta=\frac{\tau_0}{c_{44}} \tag{36}$$

Equation (36) can be rewritten in the following normalised form:

$$\Phi_1(\Xi)+\int_0^1\sqrt{\Xi\mathrm{H}}\,\Phi_1(\mathrm{H})\,\Omega(n,a,R,\Xi,\mathrm{H})\,d\mathrm{H}=\sqrt{\Xi} \tag{37}$$

where

$$\Omega(n,a,R,\Xi,\mathrm{H})=\frac{1}{\pi}\sum_{n=1,3,\cdots}^{\infty}n\left[\frac{\Gamma\left(\frac{1}{2}n\right)}{\Gamma\left(\frac{1}{2}+\frac{1}{2}n\right)}\right]^2\left(\frac{a}{R}\right)^{2n}(\Xi\mathrm{H})^{n-1} \tag{38}$$

and

$$\xi=a\Xi,\ \eta=a\mathrm{H},\ \phi_1(\xi)=\frac{\pi}{2}\frac{\tau_0}{c_{44}}\frac{\Phi_1(\Xi)}{\sqrt{\Xi}},\quad \phi_1(\eta)=\frac{\pi}{2}\frac{\tau_0}{c_{44}}\frac{\Phi_1(\mathrm{H})}{\sqrt{\mathrm{H}}} \tag{39}$$

3.2 Solution for electrically impermeable crack boundary condition

In the case of electrically impermeable crack surface condition, Eqs. (12) and (14) give the two pairs of dual integral equations (26) and (40), such that

$$\left\{\begin{array}{ll}\dfrac{1}{2\pi i}\dfrac{d}{dr}\displaystyle\int_{c-i\infty}^{c+i\infty}[e_{15}A_1(s)-\varepsilon_{11}A_2(s)]\frac{r^{-s}}{s}\tan\left(\frac{\pi}{2}s\right)ds & \\ -\displaystyle\sum_{n=1,3,\cdots}^{\infty} n[e_{15}B_1(n)-\varepsilon_{11}B_2(n)]r^{n-1}=D_0 & (|r|<a)\\ \dfrac{1}{2\pi i}\displaystyle\int_{c-i\infty}^{c+i\infty}A_2(s)\frac{r^{-s}}{s}ds=0 & (a<|r|\le R)\end{array}\right\} \quad (40)$$

It is convenient to define a new function to solve the above two pairs of dual integral equations,

$$C_k(s)=\frac{1}{2\pi i}\frac{d}{dr}\int_{c-i\infty}^{c+i\infty}A_k(s)\frac{r^{-s}}{s}\tan\left(\frac{\pi}{2}s\right)ds - \sum_{n=1,3,\cdots}^{\infty} nB_k(n)\,r^{n-1} \quad (41)$$

Using (41), Eqs. (26) and (40) can be expressed in the following form,

$$\left\{\begin{array}{ll}\dfrac{1}{2\pi i}\dfrac{d}{dr}\displaystyle\int_{c-i\infty}^{c+i\infty}A_k(s)\frac{r^{-s}}{s}\tan\left(\frac{\pi}{2}s\right)ds & \\ -\displaystyle\sum_{n=1,3,\cdots}^{\infty} nB_k(n)\,r^{n-1}=a_k & (|r|<a)\\ \dfrac{1}{2\pi i}\displaystyle\int_{c-i\infty}^{c+i\infty}A_k(s)\frac{r^{-s}}{s}ds=0 & (a<|r|\le R)\end{array}\right\} \quad (42)$$

where

$$\alpha_1=\frac{\varepsilon_{11}\tau_0+e_{15}D_0}{c_{44}\varepsilon_{11}+e_{15}^2},\quad \alpha_2=\frac{e_{15}\tau_0-c_{44}D_0}{c_{44}\varepsilon_{11}+e_{15}^2} \quad (43)$$

The solution of Eq. (42) can be obtained by introducing the new function $\psi_k(\xi)$:

$$A_k(s)=\frac{\Gamma\left(\frac{1}{2}\right)\Gamma\left(\frac{1}{2}s\right)}{2\Gamma\left(\frac{1}{2}+\frac{1}{2}s\right)}s\int_0^a\xi^s\psi_k(\xi)\,d\xi \quad (44)$$

Therefore, using Eqs. (25) and (44), the dual integral equation (42) can be rewritten as

$$\left\{\begin{array}{ll}\dfrac{d}{dr}\displaystyle\int_0^a\psi_k(\xi)\prod_1(r,s,\xi)\,d\xi & \\ -\displaystyle\sum_{n=1,3,\cdots}^{\infty}\frac{4}{\pi}nR^{-n}r^{n-1}\int_0^a\psi_k(\xi)\prod_2(r,s,\xi)\,d\xi=a_k & (|r|<a)\\ \displaystyle\int_0^a\psi_k(\xi)\prod_3(r,s,\xi)\,d\xi=0 & (a<|r|\le R)\end{array}\right\} \quad (45)$$

where $\prod_m(r,s,\xi)$ is provided in Eqs (30)~(32).

Using the same procedure in the case of electrically continuous crack condition, the unknown function $\psi_k(\xi)$ for electrically impermeable crack condition should satisfy the Fredholm integral equation of the second kind and can take the form,

$$\psi_k(\xi)+\int_0^a\psi_k(\eta)\left\{\frac{1}{\pi}\sum_{n=1,3,\cdots}^{\infty}n\left[\frac{\Gamma\left(\frac{1}{2}n\right)}{\Gamma\left(\frac{1}{2}+\frac{1}{2}n\right)}\right]^2\frac{\eta^n}{R^{2n}}\xi^{n-1}\right\}d\eta=a_k \quad (46)$$

Equation (46) can also be rewritten in the following normalised form:

$$\Psi_k(\Xi)+\int_0^1\sqrt{\Xi\mathrm{H}}\,\Psi_k(\mathrm{H})\,\Omega(n,a,R,\Xi,\mathrm{H})\,d\mathrm{H}=\sqrt{\Xi} \quad (47)$$

where $\Omega(n,a,R,\Xi,\mathrm{H})$ is the same formula as Eq. (38), and

$$\xi=a\Xi,\ \eta=a\mathrm{H},\ \psi_k(\xi)=\frac{\pi}{2}a_k\frac{\Psi_k(\Xi)}{\sqrt{\Xi}},\quad \psi_k(\eta)=\frac{\pi}{2}a_k\frac{\Psi_k(\mathrm{H})}{\sqrt{\mathrm{H}}} \quad (48)$$

4. Field Intensity Factors and Energy Release Rate

From the appropriate definitions, the expressions for the field intensity factors K_i and the energy release rate G can obtained as follows:

Electrically continuous crack surface condition

$$K_\tau=\lim_{r\to a}\sqrt{2\pi(r-a)}\,\gamma_{z\theta}(r,0)=\frac{\tau_0}{c_{44}}\sqrt{\pi a}\,\Phi_1(1) \quad (49)$$

$$K_E=\lim_{r\to a}\sqrt{2\pi(r-a)}\,E_\theta(r,0)=0 \quad (50)$$

$$K_\tau\equiv K_{III}=\lim_{r\to a}\sqrt{2\pi(r-a)}\,\tau_{z\theta}(r,0)=\tau_0\sqrt{\pi a}\,\Phi_1(1) \quad (51)$$

$$K_D=\lim_{r\to a}\sqrt{2\pi(r-a)}\,D_\theta(r,0)=\frac{e_{15}}{c_{44}}\tau_0\sqrt{\pi a}\,\Phi_1(1) \quad (52)$$

$$G=\frac{\pi a}{2}\frac{\tau_0^2}{c_{44}}\{\Phi_1(1)\}^2 \quad (53)$$

Electrically impermeable crack surface condition

$$K_{\gamma}=\lim_{r\to a}\sqrt{2\pi(r-a)}\,\gamma_{z\theta}(r,0)=\frac{\varepsilon_{11}\tau_0+e_{15}D_0}{c_{44}\varepsilon_{11}+e_{15}^2}\sqrt{\pi a}\,\Psi_k(1) \tag{54}$$

$$K_E=\lim_{r\to a}\sqrt{2\pi(r-a)}\,E_{\theta}(r,0)=\frac{c_{44}D_0-e_{15}\tau_0}{c_{44}\varepsilon_{11}+e_{15}^2}\sqrt{\pi a}\,\Psi_k(1) \tag{55}$$

$$K_{\tau}\equiv K_{III}=\lim_{r\to a}\sqrt{2\pi(r-a)}\,\tau_{z\theta}(r,0)=\tau_0\sqrt{\pi a}\,\Psi_k(1) \tag{56}$$

$$K_D=\lim_{r\to a}\sqrt{2\pi(r-a)}\,D_{\theta}(r,0)=D_0\sqrt{\pi a}\,\Psi_k(1) \tag{57}$$

$$G=\frac{\pi a}{2}\,\frac{\varepsilon_{11}\tau_0^2+2e_{15}\tau_0D_0-c_{44}D_0^2}{c_{44}\varepsilon_{11}+e_{15}^2}\{\Psi_k(1)\}^2 \tag{58}$$

where $\Phi_1(1)=\Phi_1(\Xi)|_{\Xi=1}$ and $\Psi_k(1)=\Psi_k(\Xi)|_{\Xi=1}$.

5. Numerical Examples and Discussions

In this section, several numerical examples are presented to show the influence of the crack length and the crack surface boundary conditions upon the stress intensity factor, the electric displacement intensity factor and the energy release rate. Two piezoelectric ceramics $BaTiO_3$ and PZT-5H are considered for the numerical analysis, and their material properties are listed in Table 1. The following arbitrary loads of $\tau_0=1.0(N/m^2)$ and $D_0=1.0\times10^{-3}(C/m^2)$ are used to compare the numerical results for both continuous and impermeable crack surfaces under the same conditions.

Table 1 Material properties of piezoelectric ceramics

Piezoelectric materials		$BaTiO_3$	PZT-5H
Elastic stiffness	$c_{44}(N/m^2)$	4.4×10^{10}	2.3×10^{10}
Piezoelectric constant	$e_{15}(C/m^2)$	11.4	17.0
Dielectric modulus	$\varepsilon_{11}(C/Vm)$	9.8722×10^{-9}	15.04×10^{-9}
Critical energy release rate	$G_{cr}(J/m^2)$	4.0	5.0

5.1 Field intensity factors

As given in Eqs. (49) ~ (52), all of the field intensity factors are independent of the electrical loading, if an electrically continuous crack surface condition is assumed. If on the other hand an electrically impermeable crack surface condition is assumed, intensity factors, other than the stress intensity factor, are dependent on the electrical loading, as indicated in Eqs. (54) ~ (57). Consequently, for the current central crack problem, the stress intensity factor is determined as a function of only the mechanical loading for both the continuous and the impermeable crack surface conditions. This implies that the piezoelectric properties such as piezoelectric and dielectric constants as well as the electrical loading do not have any influence upon the stress intensity factor. This is consistent with the earlier findings of the crack problems of infinite or finite geometric piezoelectric bodiessee, e.g., the works of Pak (1990), Sosa (1991), Shindo et al. (1996, 1997), and Kwon and Lee (2000, 2001).

Figure 2 shows the stress intensity factor as a function of normalised crack length a/R for the electrically continuous and impermeable crack surface conditions. The stress intensity factor increases with the increase of a/R, regardless of the electrical crack surface conditions and material properties. Assuming a crack in the unbounded piezoelectric solid : i.e., $a/R\to0$, the stress intensity factor approaches unity. This fact

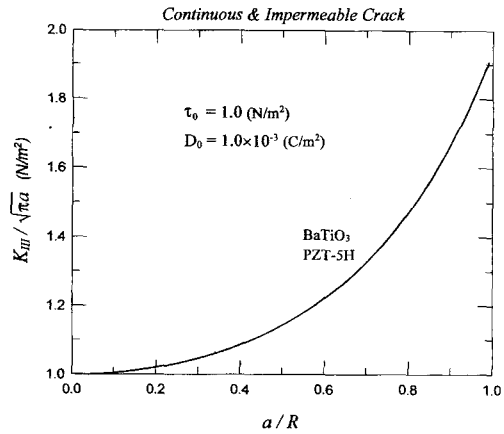

Fig. 2 K_{III} versus a/R for continuous and impermeable crack surface conditions

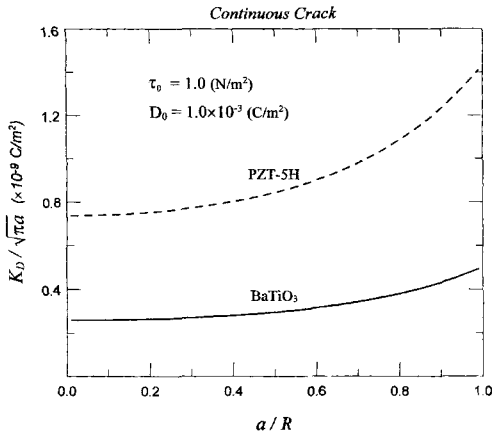

Fig. 3 K_D versus a/R for continuous crack surface condition

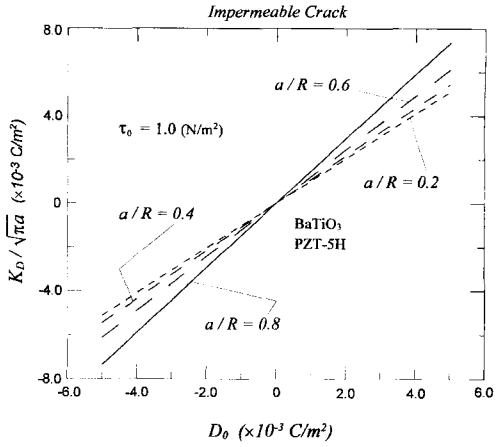

Fig. 5 K_D versus D_0 for impermeable crack surface condition

validates the present solution because it agrees with the result of Pak (1990).

The electric displacement intensity factor as a function of a/R is displayed in Fig. 3 for the continuous crack condition. In this case, the electric displacement intensity factor also increases with the increase of a/R, but its magnitude is affected by the material properties. The larger values of electric displacement intensity factor appear in PZT-5H than $BaTiO_3$.

Figure 4 shows the electric displacement intensity factor as a function of a/R for the impermeable crack condition under positive electrical loading. The electric displacement intensity factor increases with the increase in a/R, regardless of the material properties. However, the electric displacement intensity factor can decrease with the increase of a/R under negative electrical loading. This is because the direction of electrical loading affects the electric displacement intensity factor, as shown in Fig. 5. From Figs. 4 and 5, it is noted that the trend and absolute values of the electric displacement intensity factor for the impermeable crack are quite different from that corresponding to the continuous crack condition shown in Fig. 3.

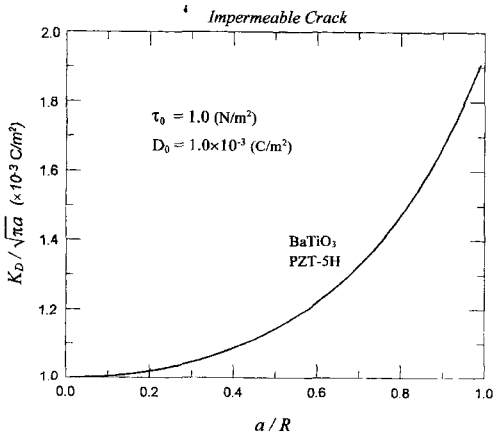

Fig. 4 K_D versus a/R for impermeable crack surface condition

5.2 Energy release rate

As given in Eqs. (53) and (58), the energy release rate for the continuous crack is only determined by the mechanical properties, while for the impermeable crack condition it is related to all of the mechanical and electrical properties. This result also agrees with the earlier findings of the crack problem in infinite or finite piezoelectric bodies see the works of Pak (1990), Sosa (1991), Shindo et al. (1996, 1997), and Kwon and Lee (2000, 2001).

Figure 6 shows the energy release rate as a function of normalised crack length a/R for theelectrically continuous crack surface condition. In this case, the numerical results show the same trend as those observed with the stress and electric displacement intensity factors; i.e., the energy release rate is influenced considerably by

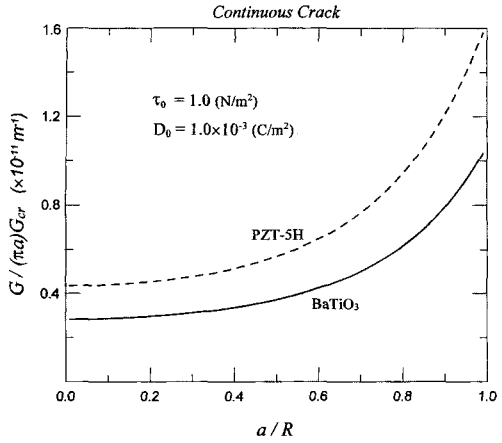

Fig. 6 G versus a/R for continuous crack surface condition

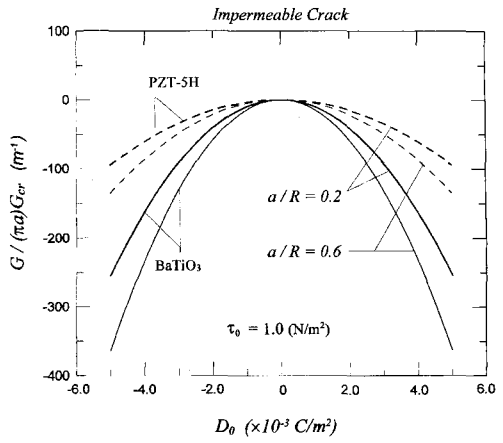

Fig. 8 G versus D_0 for impermeable crack surface condition

the change in a/R, but its magnitude is affected by the material properties. The large value appears in the case when PZT-5H is used. It is also noted that the energy release rate is always positive for the continuous crack boundary condition as the results of Shindo et al.(1996, 1997).

Figure 7 displays the energy release rate for the electrically impermeable crack surface condition under positive electrical loading. In this case, the energy release rate decreases with the increase of a/R, and is always negative. This phenomenon, which can result in retarding crack propagation, is also obtained under the negative electrical loading as shown in Fig. 8, as observed in previous studies for impermeable cracked piezoelectric material (Pak, 1990). This fact is different from the condition that the electric displacement intensity factor can be positive or negative depending upon the direction of electrical loading.

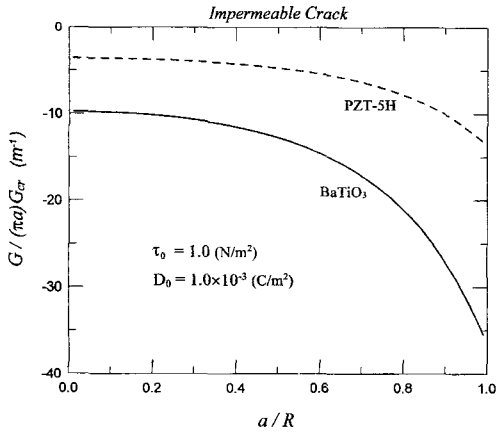

Fig. 7 G versus a/R for impermeable crack surface condition

6. Concluding Remarks

In this study, a general solution is provided for a Griffith crack in a circular piezoelectric ceramic disc of finite radius under combined anti-plane mechanical and in-plane electrical loading. The theoretical procedures and solutions are presented using Mellin transforms, Fourier series, dual integral equations and Fredholm integral equation of the second kind. Solutions are also provided to study the influence of the crack length, electrically continuous and impermeable crack surface conditions on the resulting field intensity factors and energy release. Several numerical examples are considered and the results reveal:

(i) The stress intensity factor depends on only the mechanical loading for both the continuous and impermeable crack surface conditions; it is not affected by the electric constants and/or electric loading,

(ii) The field intensity factor and the energy release rate are independent of the electrical loading when considering the electrically continuous crack surface condition. However, the energy release rate and other intensity factors,

except the stress intensity factor, depend on the electric load when considering the impermeable crack condition,

(iii) For the electrically impermeable crack surface condition, the direction of electrical loading affects the positive or negative value of the electric displacement intensity factor. While on the other, the energy release rate is always negative, regardless of the direction of electric load, which can result in retarding crack propagation.

Appendix

Equations (33) and (35) can be derived from the following special formulae of Mellin transforms (Sneddon, 1951):

$$\frac{1}{2\pi i}\int_{c-i\infty}^{c+i\infty}\frac{\Gamma(S)\Gamma(P)}{\Gamma(S+P)}X^{-s}dS = \begin{cases}(1-X)^{P-1} : 0\le X<1\\ 0 \quad : X>1\end{cases} \tag{A-1}$$

$$\frac{1}{2\pi i}\int_{c-i\infty}^{c+i\infty}\frac{\Gamma(P-S)\Gamma(1-P)}{\Gamma(1-S)}X^{-s}dS = \begin{cases}0 \quad : 0\le X<1\\ (X-1)^{-P} : X>1\end{cases} \tag{A-2}$$

By superseding $S\to\frac{1}{2}s$, $P\to\frac{1}{2}$ and $X\to\left(\frac{r}{\xi}\right)^2$, Eqs (A-1) and (A-2) are rewritten respectively as

$$\frac{1}{2\pi i}\int_{c-i\infty}^{c+i\infty}\frac{\Gamma\left(\frac{1}{2}\right)\Gamma\left(\frac{1}{2}s\right)}{2\Gamma\left(\frac{1}{2}+\frac{1}{2}s\right)}\left(\frac{r}{\xi}\right)^{-s}ds = \begin{cases}\frac{\xi}{\sqrt{\xi^2-r^2}} : |r|<\xi\\ 0 \quad : |r|>\xi\end{cases} \tag{A-3}$$

$$\frac{1}{2\pi i}\int_{c-i\infty}^{c+i\infty}\frac{\Gamma\left(\frac{1}{2}-\frac{1}{2}s\right)\Gamma\left(\frac{1}{2}\right)}{2\Gamma\left(1-\frac{1}{2}s\right)}\left(\frac{r}{\xi}\right)^{-s}ds = \begin{cases}0 \quad : |r|<\xi\\ \frac{\xi}{\sqrt{r^2-\xi^2}} : |r|>\xi\end{cases} \tag{A-4}$$

Equation (A-3) is the same as Eq. (35), and the following relations (Magnus et al., 1966) are used to obtain Eq. (33) from Eq. (A-4):

$$\Gamma\left(\frac{1}{2}-\frac{1}{2}s\right)=\frac{\pi}{\Gamma\left(\frac{1}{2}+\frac{1}{2}s\right)\cos\left(\frac{\pi}{2}s\right)}$$
$$\Gamma\left(1-\frac{1}{2}s\right)=\frac{\pi}{\Gamma\left(\frac{1}{2}s\right)\sin\left(\frac{\pi}{2}s\right)} \tag{A-5}$$

Therefore, employing (A-5), Eq. (A-4) can be expressed as Eq. (33) :

$$\frac{1}{2\pi i}\int_{c-i\infty}^{c+i\infty}\frac{\Gamma\left(\frac{1}{2}\right)\Gamma\left(\frac{1}{2}s\right)}{2\Gamma\left(\frac{1}{2}+\frac{1}{2}s\right)}\left(\frac{r}{\xi}\right)^{-s}\tan\left(\frac{\pi}{2}s\right)ds = \begin{cases}0 \quad : |r|<\xi\\ \frac{\xi}{\sqrt{r^2-\xi^2}} : |r|>\xi\end{cases} \tag{A-6}$$

Equation (34) can be determined by applying the Cauchy's residue theorem, i.e.,

$$\frac{1}{2\pi i}\int_{c-i\infty}^{c+i\infty}\frac{\Gamma\left(\frac{1}{2}\right)\Gamma\left(\frac{1}{2}s\right)}{2\Gamma\left(\frac{1}{2}+\frac{1}{2}s\right)}\left(\frac{r}{\xi}\right)^{-s}\frac{s}{n^2-s^2}ds = -\frac{\Gamma\left(\frac{1}{2}\right)\Gamma\left(\frac{1}{2}n\right)}{4\Gamma\left(\frac{1}{2}+\frac{1}{2}n\right)}\left(\frac{R}{\xi}\right)^{-n}-\frac{\Gamma\left(\frac{1}{2}\right)\Gamma\left(-\frac{1}{2}n\right)}{4\Gamma\left(\frac{1}{2}-\frac{1}{2}n\right)}\left(\frac{R}{\xi}\right)^{n} \tag{A-7}$$

The following relations are obtained from the results of Magnus et al.(1966):

$$\frac{\Gamma\left(-\frac{1}{2}n\right)}{\Gamma\left(\frac{1}{2}-\frac{1}{2}n\right)}=\frac{\Gamma\left(\frac{1}{2}+\frac{1}{2}n\right)}{\frac{n}{2}\Gamma\left(\frac{1}{2}n\right)}\cot\left(\frac{n\pi}{2}\right)=0 \tag{A-8}$$

Therefore, Eq. (A-7) can be reduced to Eq. (34):

$$\frac{1}{2\pi i}\int_{c-i\infty}^{c+i\infty}\frac{\Gamma\left(\frac{1}{2}\right)\Gamma\left(\frac{1}{2}s\right)}{2\Gamma\left(\frac{1}{2}+\frac{1}{2}s\right)}\left(\frac{r}{\xi}\right)^{-s}\frac{s}{n^2-s^2}ds = -\frac{\Gamma\left(\frac{1}{2}\right)\Gamma\left(\frac{1}{2}n\right)}{4\Gamma\left(\frac{1}{2}+\frac{1}{2}n\right)}\left(\frac{R}{\xi}\right)^{-n} \tag{A-9}$$

References

Deeg, W. F. J., 1980, *Analysis of Dislocation, Crack and Inclusion Problems in Piezoelectric Solids*, Ph.D. Dissertation, Stanford University.

Gao, C. F. and Fan, W. X., 1999, "A general solution for the crack problem in piezoelectric media with collinear cracks," *International Journal of Engineering Science*, Vol. 37, pp. 347~363.

Kwon, J. H. and Meguid, S. A., 2002, "Analysis of a Central crack normal to a Piezoelectric-Orthotropic Interface," *International Journal of Solids and Structures*, Vol. 39, pp. 841~860.

Kwon, S. M. and Lee, K. Y., 2000, "Analysis of stress and electric fields in a rectangular piezoelectric body with a center crack under anti-plane shear loading," *International Journal of Solids and Structures*, Vol. 37, pp. 4859~4869.

Kwon, S. M. and Lee, K. Y., 2001, "Eccentric crack in a rectangular piezoelectric medium under electromechanical loading," *Acta Mechanica*, Vol. 148, pp. 239~248.

Liu, J. X., Liu, Y. L., Wang, B. and Du, S. Y., 1998, "Mode III crack in the piezoelectric layer of two dissimilar materials," *Key Engineering Materials*, Vol. 145-149, pp. 1167~1172.

Magnus, W., Oberhettinger, F. and Soni, R. P., 1966, *Formulas and Theorems for the Special Functions of Mathematical Physics (3rd Ed.)*. Springer-Verlag New York Inc., p. 2.

McMeeking, R. M., 1989, "Electrostrictive stresses near crack-like flaws," *Journal of Applied Mathematics and Physics (ZAMP)*, Vol. 40, pp. 615~627.

Meguid, S. A. and Wang, X. D., 1998, "Dynamic antiplane behaviour of interacting cracks in a piezoelectric medium," *International Journal of Fracture*, Vol. 91, pp. 391~403.

Narita, F. and Shindo, Y., 1998, "Layered piezoelectric medium with interface crack under anti-plane shear," *Theoretical and Applied Fracture Mechanics*, Vol. 30, pp. 119~126.

Pak, Y. E., 1990, "Crack extension force in a piezoelectric material," *ASME Journal of Applied Mechanics*, Vol. 57, pp. 647~653.

Pak, Y. E. and Goloubeva, E., 1996, "Electroelastic properties of a cracked piezoelectric material under longitudinal shear," *Mechanics of Materials*, Vol. 24, pp. 287~303.

Park, S. B. and Sun, C. T., 1995, "Effect of electric field on fracture of piezoelectric ceramics," *International Journal of Fracture*, Vol. 70, pp. 203~216.

Qin, Q. H. and Mai, Y. W., 1999, "A closed crack tip model for interface carcks in thermopiezoelectric materials," *International Journal of Solids and Structures*, Vol. 36, pp. 2463~2479.

Shindo, Y., Narita, F. and Tanaka, K., 1996, "Electroelastic intensification near anti-plane shear crack in orthotropic piezoelectric ceramic strip," *Theoretical and Applied Fracture Mechanics*, Vol. 25, pp. 65~71.

Shindo, Y., Tanaka, K. and Narita, F., 1997, "Singular stress and electric fields of a piezoelectric ceramic strip with a finite crack under longitudinal shear," *Acta Mechanica*, Vol. 120, pp. 31~45.

Sneddon, I. N., 1951, *Fourier Transforms (1st Ed.)*. McGraw-Hill, p. 527.

Sosa, H. A., 1991, "Plane problems in piezoelectric media with defects," *International Journal of Solids and Structures*, Vol. 28, pp. 491~505.

Wang, X. D. and Meguid, S. A., 2001, "Modeling and analysis of dynamic interaction between piezoelectric actuators," *International Journal of Solids and Structures*, Vol. 38, pp. 2803~2820.

Zhang, T. Y., Qian, C. F. and Tong, P., 1998, "Linear electro-elastic analysis of a cavity or a crack in a piezoelectric material," *International Journal of Solids and Structures*, Vol. 35, pp. 2121~2149.

Zhao, M. H., Shen, Y. P., Liu, Y. J. and Liu, G. N., 1997, "Isolated cracks in three-dimensional piezoelectric solid. Part II : Stress intensity factors for circular crack," *Theoretical and Applied Fracture Mechanics*, Vol. 26, pp. 141~149.